63-3

63-927-534-R1

WESTINGHOUSE ELECTRIC CORPORATION

RESEARCH LABORATORIES

WEBBED DENDRITIC SILICON SOLAR CELL RADIATION EFFECTS INVESTIGATION

QUARTERLY PROGRESS REPORT

FOR PERIOD

January 15 - April 15, 1963

CONTRACT AF 33(657)-10527
PROPRIETARY CLASS 3

WESTINGHOUSE RESEARCH LABORATORIES
PITTSBURGH • PENNSYLVANIA

WESTINGHOUSE RESEARCH LABORATORIES

Sensitivity Categories* for Technical Documents

PROPRIETARY CLASS 1 . . .	Strictly limited. Cannot under any circumstances be distributed outside the Company. Inside the Company, recipient must have a specific need for the information in the conduct of his assigned responsibilities.
PROPRIETARY CLASS 2 . . .	Distribution only within the Company. Copies of such documents cannot be either given or shown to anyone outside the Corporation except (1) licensees (with Associated Companies' approval) and (2) the government in proposals for contracts.
PROPRIETARY CLASS 3 . . .	Unlimited distribution, both inside and outside the Company.

*Determined by the author with the approval of his department manager. For further information, see "Guide for Classification and Distribution of Internal Communications."

Research Report 63-927-534-R1
Proprietary Class 3

WESTINGHOUSE ELECTRIC CORPORATION

RESEARCH LABORATORIES

WEBBED DENDRITIC SILICON SOLAR CELL RADIATION EFFECTS INVESTIGATION

QUARTERLY PROGRESS REPORT FOR THE PERIOD January 15 - April 15, 1963

K. S. Tarneja[1]
R. V. Babcock[2]
R. D. Lamb[1]

The Research and Development reported in this document has been made possible through support and sponsorship extended by the Flight Accessories Laboratory of the Wright Patterson Air Force Base, Ohio, under contract number AF 33(657)-10527. It is published for technical information only and does not necessarily represent recommendations or conclusions of the sponsoring agency.

[1]Special Products Section, Westinghouse Electric Corporation, Youngwood, Pa.

[2]Research Laboratories, Westinghouse Electric Corporation, Pittsburgh, Pa.

Foreword

The studies presented began in January 1963 and represent the efforts until April 15, 1963. Studies presented here were carried on under the direction of Mr. R. K. Riel, Manager, Special Products Section, Westinghouse Electric Corporation, Youngwood, Pa. and Dr. K. H. Sun, Manager, Radiation and Nucleonics Laboratory, Research Laboratories, Pittsburgh, Pa. Other contributors to this report were Messrs. E. Stonebraker and L. H. Garrison, of Westinghouse Electric Corporation, Youngwood, Pa., and P. E. Felice, of the Research Laboratories. Their help is gratefully acknowledged.

The work covered by this report was accomplished under Air Force Contract 33(657)-10527, monitored by Mr. Joseph F. Wise, ASRPP-20, Static Energy Conversion Branch of the AF Aero-Propulsion Laboratory, but this report is being published and distributed prior to Air Force review. The publication of this report, therefore, does not constitute approval by the Air Force of the findings or conclusions contained herein. It is published for the exchange and stimulation of ideas.

ABSTRACT

This report discusses initial work toward maximizing the radiation resistance of silicon webbed dendritic solar cells. Design considerations, techniques for fabricating cells of 1 Ω cm resistivity, and steps preparatory to radiation damage study are presented. Efficiencies as high as 12.4% have been achieved on solar cells made from 1 Ω-cm n-type silicon webbed dendrites.

TABLE OF CONTENTS

I. Introduction

With recent advances in space, solar cells have gained considerable importance. The solar cell is a semiconductor device which will convert radiant energy into electrical energy. At present, the so-called semiconductor solar cell provides the highest available efficiency in converting solar radiation energy to useful electrical output. This cell is essentially a large area diode with an extremely shallow p-n junction (depth of the order of 1 micron). The cell is shown schematically in Figure 1. The carrier concentration gradients at a p-n junction provide the driving force to maintain a "built-in" junction field. When hole-electron pairs are generated by conversion of the energy of light quanta absorbed in the crystal, minority carriers diffusing into the junction transition region are accelerated by the junction field and are thereby "collected." The result of this disturbance of the dark conditions of equilibrium is a photovoltaic voltage which is capable of driving current through an external load, and also causes an internal shunt current to flow across the junction in the forward direction. The junction depth is made small so that the greatest possible proportion of photo-generated minority carriers may diffuse into the junction transition region before being lost to recombination.

Silicon solar cells are ordinarily prepared from grown cylindrical single-crystals of silicon, which are cut into thin rectangular plates, lapped, then formed into solar cells. By the process of webbed dendritic growth, long thin strips of silicon can be grown directly. This eliminates several steps ordinarily required for the fabrication of solar cells and

reduces silicon wastage. The process of dendritic growth and the development of webbed dendritic solar cells are discussed in other reports.[1]

A primary limitation on the use of solar cells in space is radiation damage from energetic protons and electrons. The object of this study is to find the particular structure and fabrication procedure which maximizes the resistance of webbed dendritic silicon solar cells to damage by the radiation fluxes found in space.

---

[1] Research on Improved Solar Generator, Tech. Doc. Report No. ASD-TDR-62-1000, contract AF 33(657)-7649.

II. Preparation of Solar Cells

The immediate objective of this study is to find a particular cell structure and fabrication procedure which maximizes the resistance to damage by 2 MeV* electrons. Of the several parameters expected to affect radiation resistance, we will vary some and minimize, or hold constant, others. Oxygen content, general purity, and initial dislocation concentration will be minimized as far as practicable. Contact resistance will be held at a constant value, hopefully negligible, by use of a standard contact structure. The parameters to be varied, in order of their expected importance to radiation resistance, are:

1) Resistivity type
2) base-resistivity
3) diffusion depth
4) time-temperature profile of diffusion
5) temperature during irradiation
6. dose rate.

A tentative schedule outlining the order in which various combinations of the above parameters will be studied was included in the first monthly status letter.

During this quarter solar cells were prepared from n-type silicon webbed dendrites of 1.0 Ω-cm resistivity, with junction depths of 1μ, 1/2μ, and 1/3μ. Boron (a p-type dopant) was diffused into the n-type

---

*One MeV electrons may be used instead; this decision will be made shortly. All equipment and technique described is appropriate to either electron energy.

base layer, using BCl_3 as a boron source. The flow diagram for the preparation of solar cells from webbed silicon dendrites is shown in Figure 2.

A. Material Evaluation

In order to have a controlled process it is very important to evaluate the material completely before any solar cells are fabricated. The webbed dendrites were received in 12" lengths, and resistivity was measured at 1/2" intervals along both sides down the length of the webbing, using the two probe resistivity measurement technique. The resulting resistivity values are shown in Table I. It is seen from Table I that there is no significant change in resistivity along the length of the strip. Dislocation etch pit density is then measured on three small pieces taken from each end and the center of each strip. Dislocation densities on these pieces were in the range of 0-5,000 pits/cm^2. Equipment is being set up to measure the minority carrier lifetime on the silicon webbed material. Thus properties such as resistivity, dislocation density and lifetime are measured and recorded prior to the fabrication of solar cells.

A program has been initiated to determine the oxygen content of silicon webbed dendrites. Initially samples with dendrites, without dendrites, and with sandblasted surfaces were submitted for oxygen analysis. The results have not been evaluated completely. Further evaluation will be made and the results included in later reports.

B. Pre-Diffusion Cleaning

Webbed silicon dendrites are cut into 2 cm lengths, mounted on a flat plate with wax, and their surfaces sandblasted. The sandblasting causes surface damage which is removed by etching prior to diffusion.

C. Diffusion

The solar cell is a one-junction device whose parameters are critically dependent upon certain physical properties such as carrier concentration in the highly doped surface region and minority carrier lifetime. These requirements place strong emphasis on the proper choice of a process for junction formation. A vapor diffusion process satisfies most requirements. This process consists of heating webbed silicon dendrites to a pre-determined temperature while passing vapors of boron over them for a preset time. In the case of boron, a surface film is formed by chemical reactions between silicon and boron tri-chloride;

$$4BCl_3 + Si \rightarrow 4B + 3\ SiCl_4.$$

Silicon acts as a reducing agent and a small amount is lost during reaction. This is in a sense an etching procedure and maintains a clean surface until the proper diffusion temperature is reached. This vapor diffusion process also preserves lifetime.

An approximate diffusion time may be calculated[2] using the relation derived in Appendix I,

$$x = 7\sqrt{Dt}\ ,$$

where x = diffusion depth in cm,

D = diffusion coefficient, a function of temperature, in cm^2/sec,

t = diffusion time in seconds.

---

[2] Research on Improved Solar Generator, Scientific Report No. 1, contract AF (616)-6612.

Diffusion runs of various durations were made to achieve junction depths of 1μ, 1/2μ, and 1/3μ in n-type silicon webbed dendrites. Figure 3 shows the diffusion furnace used for these runs. Junction depths are usually determined using 5^{o} angle lapping followed by staining. The staining technique consists of etching in nitric and HF acid combinations. For boron diffused solar cells, it was found that the samples to be analyzed for junction depth should be cleaned prior to angle lapping to remove any insulating layers produced during diffusion. Furthermore, since solar cells do not have highly polished surfaces, more accurate diffusion depths can be determined by inserting a chemically polished slice with each diffusion run. Angle lapping of these slices yields satisfactory results.

D. Post-Diffusion Techniques

After diffusion, the silicon webbed dendrite has a glassy boron diffused layer on the exposed side and an extremely shallow diffused layer on the masked (bottom) side. Both these sides have to be cleaned to remove the opaque glass from the top surface and the unwanted junction from the bottom. The boron glass is removed by etching in acids. Usually the back junction is removed by sandblasting. These processes provide satisfactory surfaces for contacting.

E. Contacting and Etching Techniques

In the fabrication of high efficiency solar cells, the formation of ohmic contacts having high electrical conductivity, without damaging the device, is one of the difficult problems. Grid structure contacts distributed over the entire diffused layer are used in order to facilitate collection of holes

and, consequently, to lower the series resistance of the cells. Grid structure contacts were made on the p-layer using photo-resist techniques. After the grid pattern had been applied, the units were nickel plated by an electroless technique. Acid etching was then used to separate p and n layers and to reduce leakage current.

The solar cells were mounted on metal plates in order to provide good thermal contact to the aluminum heat sink to be used during irradiation. Aluminum plates 0.8 cm x 3.5 cm were designed with a terminal for the top contact of the cell. To facilitate soldering to the Al surface, a 0.8 cm x 2 cm area was sprayed with copper using plasma jet techniques. Figure 4 shows the metal plates after spraying and addition of the terminal. Figure 5 shows the solar cell after dip soldering to the plate.

F. Testing Techniques

For each fabricated cell, the following quantities are measured: V_{oc}, I_{sc}, V_m, I_m, P_m, R_{Lm}, CF, η, J, R_{se}, and R_{sh}. These measurements are made under tungsten lamps, Westinghouse DXC 500 watt, operated at 3400°K color temperature, and under a light intensity of 140 mw/cm^2. The test apparatus which will soon be in use is shown in Figure 6. The arrangement currently being used is pictured in Figure 7.

The lifetime of minority carriers in the base region is being measured by the well known "diode recovery" technique. A Tektronix scope with type S plug in unit is used for this measurement. The lifetime measurement is done on 90 mil diameter dice cut from the centers of fabricated cells. The lifetime of a batch is characterized by that of one of its cells. The lifetime measuring equipment is shown in Figure 8.

A Perkin-Elmer Model 12-C spectrophotometer (shown in Figure 9), modified as described below, has been obtained during this period. Spectral response curves are routinely measured on this instrument; a sample curve is shown in Figure 10. This instrument provides an automatic system for measuring the spectral response of solar cells from approximately .22 microns to 2.6 microns. Energy from one of two sources (hydrogen or tungsten) is directed into a special monochromator in which a SiO_2 prism is used. The monochromatic exit slit energy is divided by a beam splitter--one portion going to the reference thermocouple and the remainder going to the detector under test. The reference thermocouple is part of a servo loop which controls the slits so that the exit slit energy remains constant.

The solar cell I_{sc} is amplified and displayed on a L and N strip chart recorder. Since the energy striking the solar cell is constant, any variation in output sensitivity is due to the solar cell itself. Scanning wavelength, therefore, gives a plot of sensitivity vs wavelength; i.e., the spectral response of the solar cell.

The system is also capable of measuring the spectral response of various light sources. One of the existent light sources (tungsten or hydrogen) may be replaced with an unknown source of light. The beam splitter may be replaced with an Al front surface mirror and the energy from the reference thermocouple may be recorded, thus providing the relative intensity distribution of an unknown light source. (The slits may be set at constant width and the slit servo de-energized.)

III. Radiation Damage Studies

The mechanism of radiation damage to the operating characteristics of silicon solar cells consists almost entirely of the introduction of recombination centers into the base material, which decreases the minority carrier diffusion lengths. Because the optical absorption constant in silicon decreases sharply with increasing wavelength over the visible region, the longer wavelength light is absorbed deeper in the base region of the cell, and must diffuse farther to be collected. Consequently, the effect of radiation damage is to reduce the long wavelength response of the cell, the effect extending to progressively shorter wavelengths as irradiation progresses.

To a first approximation, any type of bombarding particle introduces recombination centers at a given rate, and the most resistant type of cell structure will be that structure whose output characteristics decline least due to the introduction of a given concentration of recombination centers. Consequently, the relative damage resistance of different cell types should be similar regardless of the nature of the bombarding particle. Of course, the recombination centers introduced by bombarding particles of different types and energies will differ somewhat in their nature; thus the cell structure that is most resistant to one radiation flux will not always be most resistant in a flux of different composition. In this investigation we employ a single type of radiation (2 MeV or 1 MeV electrons) and accurately compare the radiation resistance of different cell structures until the most damage resistant structure and fabrication procedure has been developed. The optimization procedure requires precise determination of relative damage rates

among a large number of different solar cell structures. The achievement of this precision requires;

1) good control of starting material,

2) reproducible fabrication techniques,

3) reproducible electron dosimetry, and

4) precise measurement of efficiencies.

A prerequisite to 1) and 2) is a unified, continuous production effort. A check on 1) is obtained by irradiating duplicate samples from each production run. A check on 2) is obtained by irradiating sets of samples from each of several production runs together. Electron dosimetry is accomplished by an especially designed Faraday cup which has a sensitive area exactly equal to the area (and shape) of the sample solar cells. This Faraday cup, and the cells under test, are oscillated through the electron beam in such a way that each solar cell, and the Faraday cup, spend equal times in any particular portion of the beam pattern. Thus the current from the Faraday cup, integrated over the entire irradiation, is equal to the total electron current intercepted by each cell, in spite of changes with time of the intensity, or intensity distribution, of the electron beam.

A. Method of Irradiation

The electron beam from a 2 MeV Van de Graaff generator, defocused to a spot several inches in diameter, is allowed to fall on a conveyer belt, as shown in Figure 11. Nine solar cells (triplicate samples from each of three production runs, all with the same nominal characteristics) are accurately centered about the axis of motion of the conveyer belt. The Faraday cup is

mounted with its collimating hole also centered about the axis of motion and at the same level, so that its sensitive area occupies a position exactly equivalent to the position of any solar cell. With the electron beam on, the conveyer belt is moved back and forth at constant speed over a sufficient length of travel that all ten units pass completely out of the electron field at each end of the travel. If the beam pattern is constant, the total integrated flux per unit width (along the direction of travel) is the same for all ten units after one pass. If the gradient of beam intensity is small over 2 cm perpendicular to the direction of motion, the integrated flux per unit area is also the same for each unit. If the beam is very non-uniform over this 2 cm, each unit must have the same length in order to receive exactly the same integrated flux. If the units are well alligned and of the same length, the integrated flux through each after a large number of passes will be identical, despite variations in beam intensity and distribution.

The nine cells are mounted on a sample holder which can maintain them at a chosen constant temperature between -75°C and +75°C, either during irradiation or during measurement. The cells are not demounted during the duration of damage testing. The cells are irradiated for different periods, so that the total exposure, as indicated by the total charge entering the Faraday cup, increases by a factor of 3 (or 3.33...) at each interval. Illuminated and dark current-voltage (I-V) characteristics are measured at each interval.

B. Measurements During Damage Testing

In Section II, the measurements to be made before and after irradiation were enumerated. The essential characteristic to observe during the course of irradiation is the illuminated I-V characteristic, from which the efficiency is determined. At each interval between irradiations two illuminated I-V curves will be measured for each cell; using 3400°K black body radiation, and with the same light source filtered through 1/2" of plexiglass and 3 cm of de-ionized water. Dark I-V curves will also be measured at some intervals.

Light I-V curves are measured in a relatively conventional manner. The 3400°K tungsten lamp is maintained at constant intensity above a stage holding two IRC calibrated solar cells and the nine sample cells. The lamp can be moved toward or away from the stage until the output of the standard cells indicates an intensity equivalent to the air mass zero solar intensity of 140 mw/cm^2. Each sample cell is then successively placed in position for measurement by a perpendicular motion of the stage. An I-V curve, covering the power quadrant and parts of the two adjacent quadrants, is automatically plotted by an x-y recorder in about six seconds. Appropriate signals to calibrate the measurement circuitry are simultaneously plotted by the recorder. After each sample cell has been measured, the filter is interposed between light source and samples, the stage is repositioned to restore equivalent solar intensity, and the measurement process is repeated.

Dark I-V curves are obtained from the same equipment with the light source extinguished. The purpose of taking these curves is to estimate the

series resistance of the cell from the forward characteristic, and to find the shunt resistance from the reverse characteristic.

The 3400°K light source, although it is stable and provides an accurately known frequency distribution, produces much more long wavelength light than the roughly 6000°K solar spectrum. This leads to the by now well known effect that the rate of radiation damage is overestimated by testing with 3400°K light because of the more rapid loss in cell response at the longer wavelengths.

The filtered light source has been found by other workers to indicate rates of decrease in solar cell efficiency with irradiation that match the rates measured in sunlight rather well. Although the filter does remove long wavelengths, the frequency distribution of the filtered source by no means matches that of the sun. It must be remembered that the agreement with sunlight measurements of radiation damage rates is to some extent empirical. The observed damage rates can be checked at two points by combining the spectral response data taken before and after irradiation with the unfiltered tungsten efficiencies to estimate the solar efficiencies at these two points.

C. Equipment

The sample holder has four major functions: 1) to hold up to eleven solar cells in accurate, reproducible positions for irradiation or measurement, 2) to maintain the cells at a constant temperature (within about 2°C) in the range -75°C to +75°C. 3) To serve, together with the cell material, as an infinite, homogeneous electron stopping medium, so

that the electron backscatter flux will be uniform and known, and 4) to provide a dry inert atmosphere over the cells during low temperature measurement.

The sample holder, which is shown in cross section in Figure 12, is basically a well insulated ice chest with a top surface of 1/4" thick aluminum. The cells, themselves backed by 1/8" aluminum bases, are screwed to the top surface. This provides a uniform stopping medium of relatively low atomic number (Al = 13, Si = 14) which minimizes the amount of back-scattered electron flux. A thin plastic cover (1/16" plexiglass) can be sealed to the wooden rim to contain an atmosphere of dry nitrogen gas, which will prevent frosting of the cold cell surfaces during low temperature measurements. The ice chest can be filled with carbon dioxide ice or ammonia ice to maintain cell temperatures of -75°C, with liquid ammonia to provide -32°C or with water ice to give 0°C. One filling is sufficient for several hours. Two 50 watt cartridge heaters embedded in the aluminum top allow operation at any temperature from ambient to +75°C. Several thermocouples are embedded in the aluminum top and in a dummy solar cell baseplate. All power and signal connectors are mounted on the sample holder, which can be unplugged for rapid transfer from irradiation to measurement locations. The metal base plate is notched to match an indexing system in the power curve measurement apparatus which allows any solar cell to be accurately placed with respect to the light source.

Electron flux measurement is accomplished by means of a Faraday cup of special construction, shown in cross section in Figure 13. The cup consists essentially of three closed concentric shells; of metal, insulator, and metal. The outer shell consists of 1/8" brass and carries a collimating plate of 0.050" gold with an appropriate beam hole. A very thin metallic coating on the upper surface of the mica plate completes the electrical enclosure. Three collimating plates are provided; one has a 2 cm by 0.8 cm beam hole which matches the solar cell area, one has a 2 x 2 cm beam hole which can also simulate the solar cell area if properly oriented, and the third has no hole and is used to check current leakage during irradiation.

The insulating shell consists of ten mil polystyrene molded to the inner brass shell, plus two mil vinyl tape. The insulating circuit is closed in the vicinity of the beam hole by a 0.7 mil mica window, which is coated with silver paint on both sides to close the two conducting shells. The total thickness of the painted mica window is 6.7 mg/cm^2. The inner conducting shell consists of 1/8" brass, with a 1/4" aluminum insert in the bottom to minimize electron backscatter.

In operation, the Faraday cup is so placed on the conveyer belt that the collimator hole traverses exactly the 2 cm wide path traversed by each sample solar cell. Either collimating plate can be used, with the 2 cm dimension perpendicular to the direction of travel. The current collected by the inner shell is integrated over the entire irradiation.

The accuracy of the integrated current reading depends upon several factors:

1) Current leakage through the insulating shell--this should be negligible.

2) Passage through the mica window of energetic secondary electrons ejected from the edges of the collimator--this effect has probably been made negligible by chamfering the edges of the collimator at 10° so that it is narrowest at the face toward the electron beam source.

3) Uncertainty of the effective area of the beam hole--since some electrons can pass through the thinner portions of the chamfered gold edges the effective locations of the edges are altered by about 5 mils. This leads (for 2 MeV electrons) to an increase in the effective area of the hole of about 2% for the 2 cm by 2 cm collimator and about 3% for the smaller collimator. These increases are less than half as large if 1 MeV electrons are used. For an exactly parallel electron beam the increases could be estimated, but some uncertainty is unavoidable because of the variations in incident electron direction. For this reason, as well as the uncertainty in measuring the physical (i.e., optical) hole areas, the effective hole area is considered uncertain to 3%.

4) Escape of electrons backscattered from the bottom of the cup--this can be estimated and amounts to about 0.5%.

5) Escape of electrons backscattered by the mica window--about 0.6%.

Although some correction can be made for all of these factors, the current measurement at the Faraday cup will be uncertain to about 3%. The errors due to misalignment between the paths of the collimating hole and the paths of the sample cells will probably amount to more than this, unless the

electron beam pattern is extremely uniform. The overall measurement of electron intensity should be accurate to much better than 10%.

The circuitry associated with I-V characteristic measurements is shown in Figure 14. The circuit is basically a variable load resistance placed across the solar cell contacts, with cell voltage and IR drop across a 5Ω resistor being applied directly to the inputs of a Mosely "Autograf" x-y recorder. The one-turn variable potentiometer is driven by a 10 RPM motor so that a full I-V curve is plotted in six seconds. A four volt battery and two 10Ω resistors convert the variable resistance into a voltage divider which causes the power curve to be extended slightly into the two adjacent quadrants, thus assuring unambiguous measurement of I_{sc} and V_{oc}.

When the two 10Ω resistors are shorted out, the dark I-V curve is drawn between the limits of -2 volts and +280 ma. The calibration circuit causes the potential across a 2.2 μf capacitor to rise from zero to the 1.34 volts supplied by the mercury cell. This causes a straight line to be drawn in the power quadrant of the illuminated I-V curve from the origin to (0.5 volt, -50 ma). All of the circuitry is reversible in polarity, so that both n-type and p-type cells can be measured with their bases grounded.

IV. Future Program

Testing of the resistance to electron damage of the 1Ωcm n-type base cells will begin shortly. Cells from n-type webbed dendrites of 5, 10, and 20Ωcm will be fabricated and tested under irradiation. Fabrication of p-type base cells having base resistivities of 1, 5, 10, 20, and 25Ωcm will begin concurrently, and these cells will be tested after the high resistivity n-type base cells. After comparing these test results, the study of n-type base cells outlined in the tentative schedule may be curtailed in order to concentrate on p-type base cell structures.

APPENDIX I

Calculation of p-n Junction Depths

It is assumed that the diffusion of boron into silicon under the experimental conditions is given by the complementary error function,

$$c(x) = c_o \operatorname{erfc} x/2L, \tag{A}$$

where

$$L = (D\,t)^{1/2} \tag{B}$$

is the diffusion length and c_o is the surface concentration of diffusant.

This expression for the distribution of diffusant is an approximation. The actual distribution function is somewhat different, since the formation and volatilization of $SiCl_4$ from the exposed faces of the silicon produces a recession of the silicon surface with a small velocity. As pointed out in Section II of the report, the removal of silicon proceeds according to the reaction

$$3Si + 4BCl_3 = 4B + 3SiCl_4\uparrow \quad . \tag{C}$$

Referring to Eq. (A), we can readily evaluate c(x) at the junction from the following well-known relationship:

$$\sigma_n = n_D\, e\mu_n = c(x_j)\, e\mu_n \,, \tag{D}$$

where the mobility μ_n is a function of the conductivity of the base silicon, σ_n. Now c_o may vary from 10^{19} to 10^{22}/cc, the highest possible value being the design objective. The Table below gives x_j in terms of L for various values of c_o and base resistivities ρ_n as calculated from Eq. (A). Tables of the complementary error function may be used for this evaluation, but it

is more convenient to use the complementary error function graph paper which we have designed for use in the investigation of diffusion processes (see the following page).

Table A. Values of Junction Depth in Terms of Diffusion Length, for erfc Distribution

c_o (cm^{-3})	ρ_n	x_j	ρ_n	x_j	ρ_n	x_j
10^{19}	0.3	4.2L	1	4.7L	3	5.2L
10^{20}	0.3	5.1L	1	5.6L	3	6.0L
10^{21}	0.3	5.9L	1	6.3L	3	6.7L
10^{22}	0.3	6.6L	1	7.0L	3	7.3L

For typical cases, it may be seen that the approximation

$$x_j = 6L \qquad (E)$$

may be chosen as a suitable guide to device design, in view of the uncertainty in the value of the diffusion coefficient, D. It is convenient to express Eq. (E) in a modified set of units, for laboratory calculations. Insertion of the appropriate conversion factors yields the following useful approximation:

$$x_m = 0.006\ (D_{13} t_m)^{1/2} \ , \qquad (F)$$

where

x_m = junction depth in mils,

$D_{13} = D \times 10^{13}$,

D = diffusion coefficient (for boron in silicon, $D = 1 \times 10^{-13}$),

t_m = diffusion time in minutes.

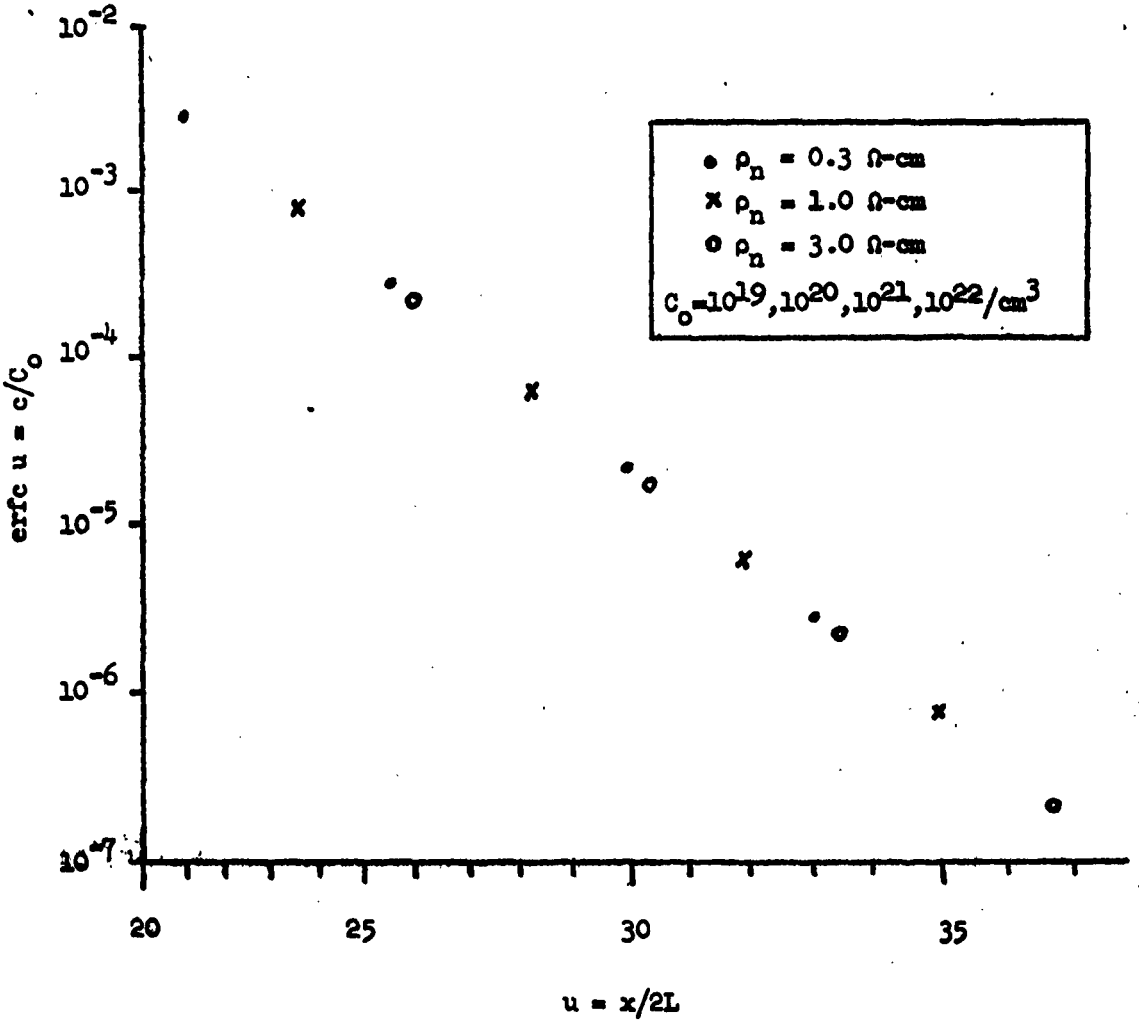

Complementary Error Function Plot

TABLE I

Reading Position	Resistivity ohm-cm	Reading Position	Resistivity ohm-cm
A_1	1.008	A_2	1.025
B_1	1.025	B_3	1.092
C_1	1.058	C_2	1.092
D_1	1.092	D_2	1.142
E_1	1.092	E_2	1.092
F_1	1.092	F_2	1.092
G_1	1.092	G_2	1.042
H_1	1.092	H_2	1.042
I_1	1.042	I_2	1.042
J_1	1.025	J_2	1.058
K_1	1.025	K_2	1.042
L_1	1.042	L_2	1.042
M_1	1.092	M_2	1.042
N_1	1.092	N_2	1.042
O_1	1.075	O_2	1.042
P_1	1.025	P_2	1.042
Q_1	1.025	Q_2	1.042
R_1	1.075	R_2	1.042
S_1	1.025	S_2	1.042
T_1	1.025	T_2	1.042
U_1	1.109	U_2	1.075
V_1	1.058	V_2	1.075
W_1	1.075	W_2	1.075

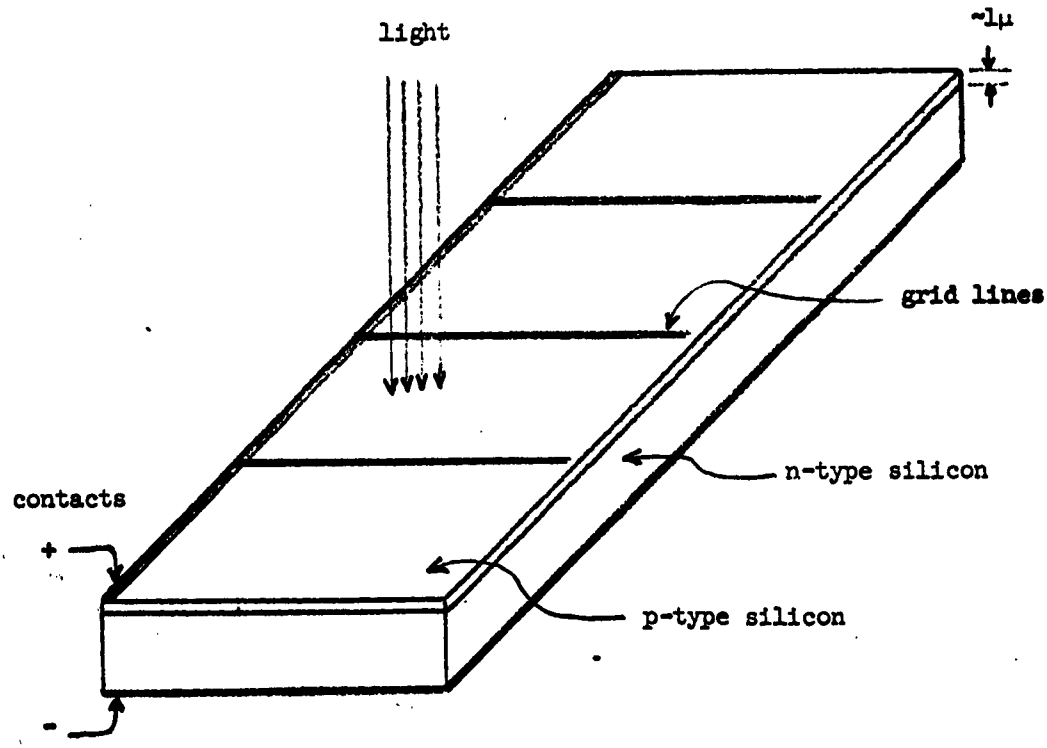

Figure 1. Sketch of Solar Cell

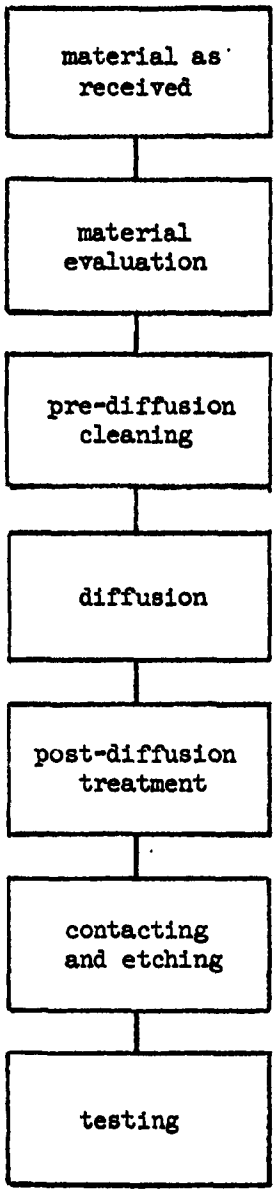

Figure 2. Flow Diagram of Solar Cell Processing

Figure 3

Diffusion Furnace

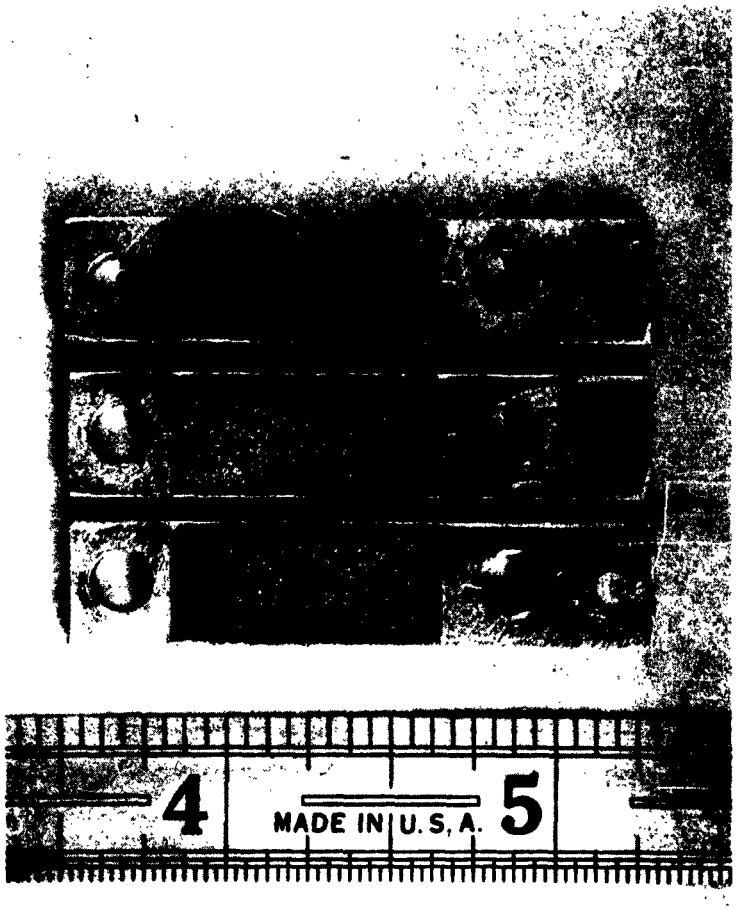

Figure 4

Metal Plates with Terminal
on Top for the Contact

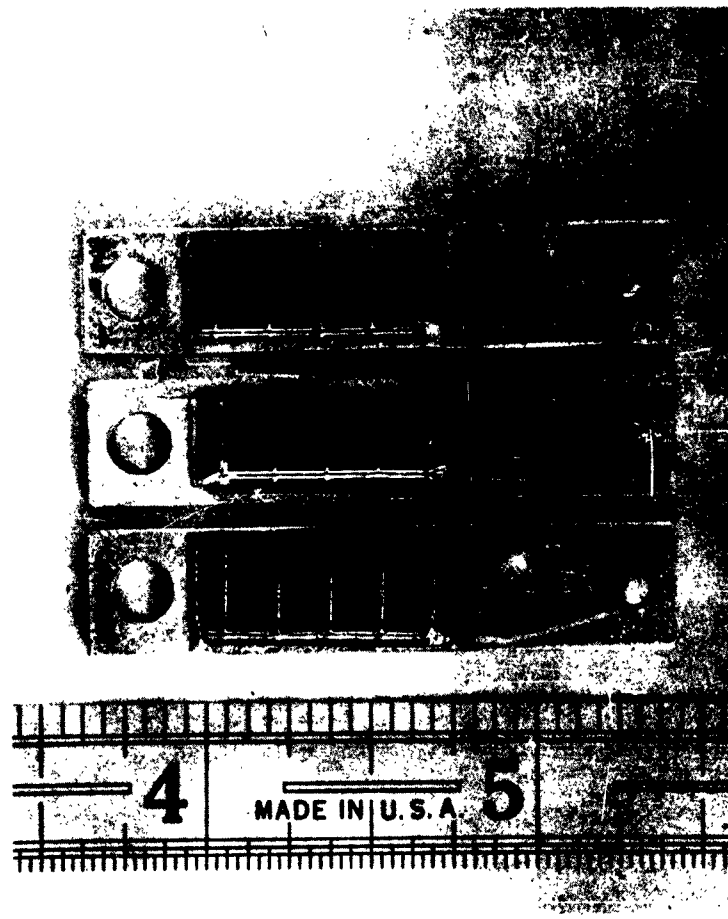

Figure 5

Metal Plates with Solar
Cells Mounted on These Plates

Figure 6

Efficiency Measurement
Equipment

Figure 7

Efficiency Measurement
Tester

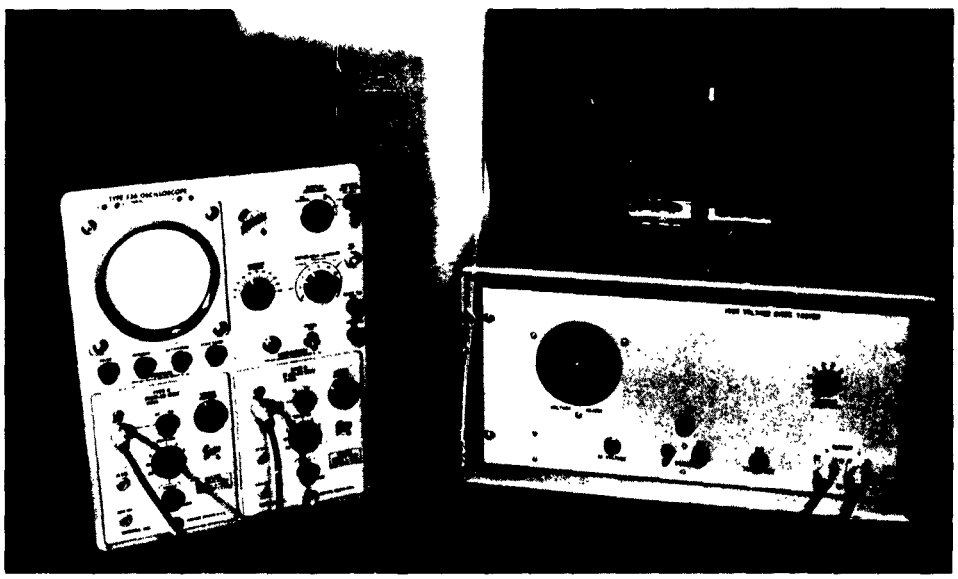

Figure 8

Lifetime Measuring
Equipment

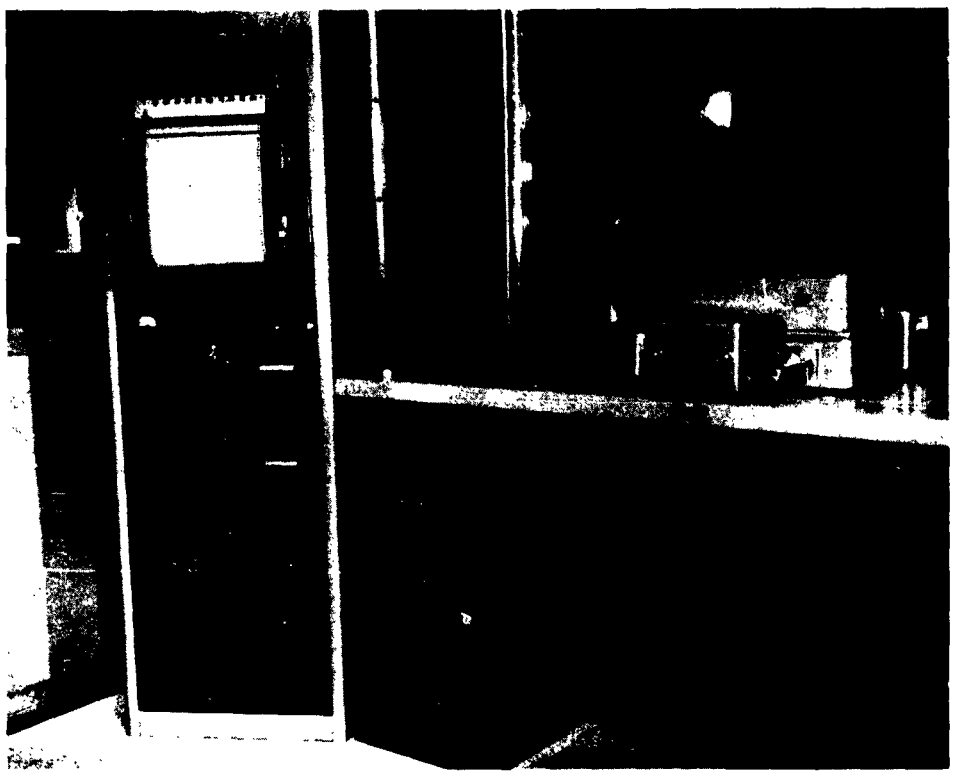

Figure 9

Spectral Response
Measuring Apparatus

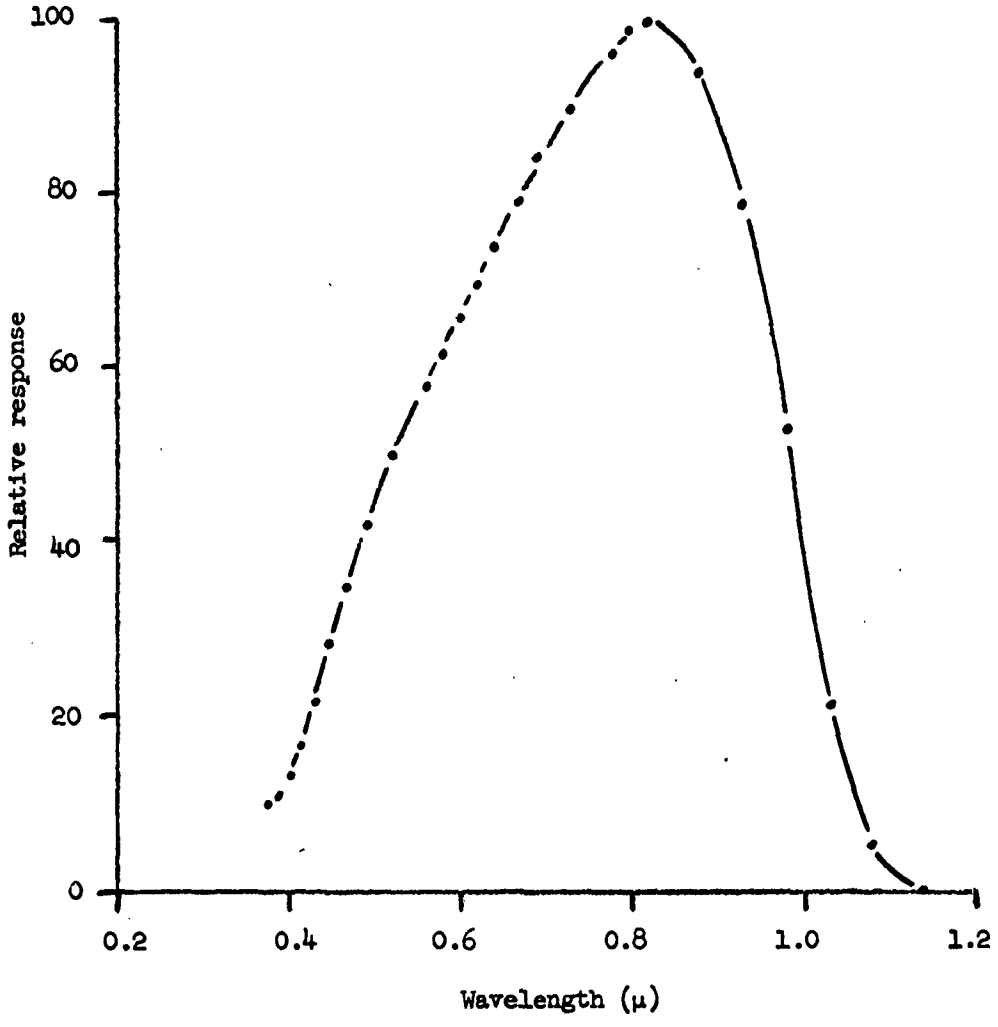

Figure 10. Spectral Response of Cell R11#3

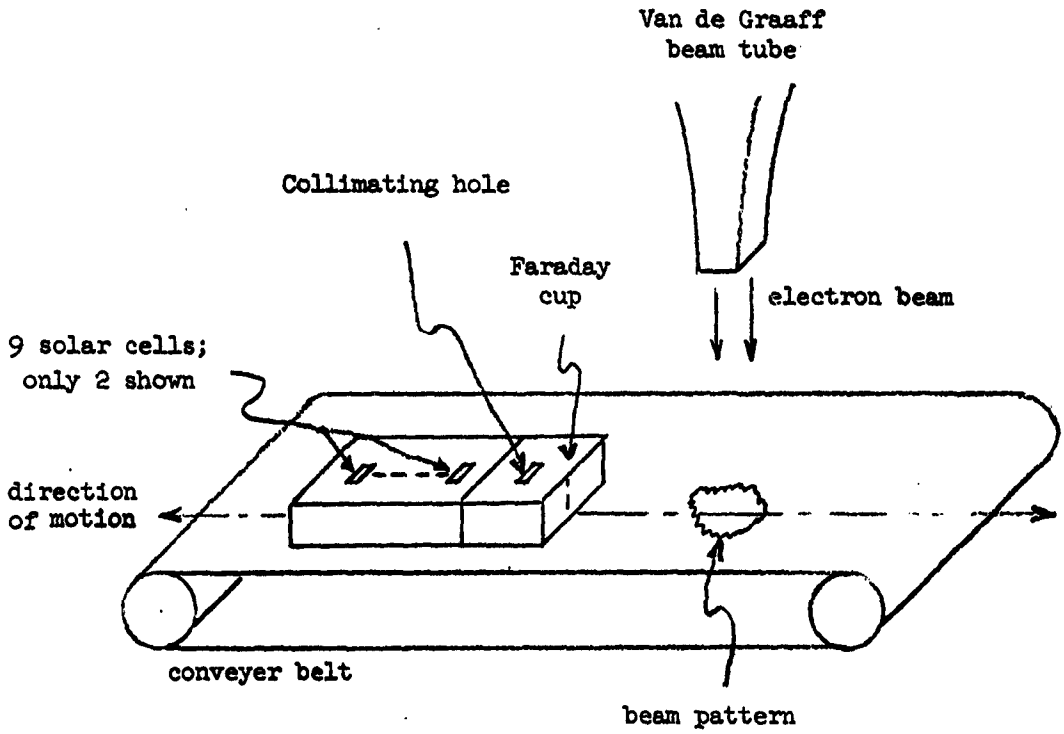

Figure 11. Sketch of Irradiation Geometry. As the conveyer belt oscillates at constant speed, all solar cells and the collimation hole receive the same integrated electron flux.

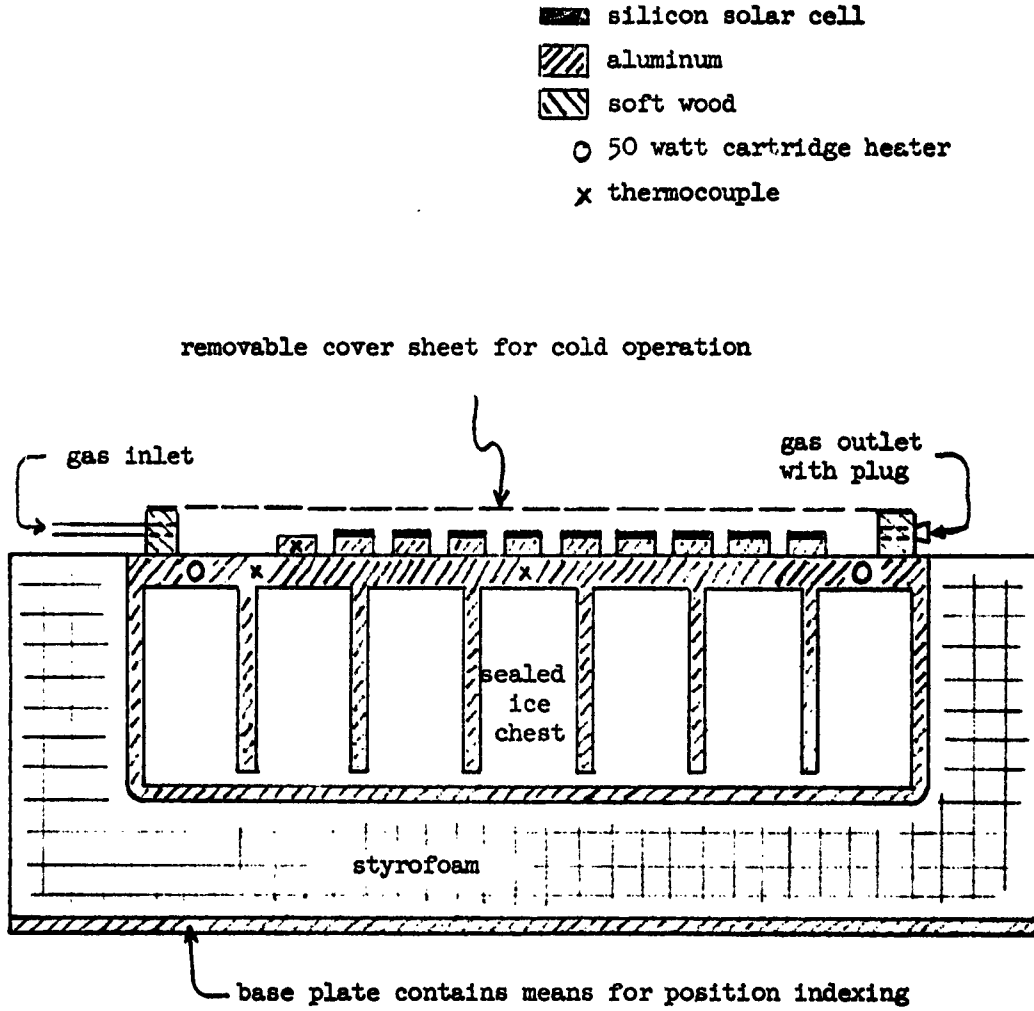

Figure 12. Cross Sectional View of Sample Holder to 2/3 Scale. Nine solar cells and a dummy containing a thermocouple are in place. Construction details and electrical connections are not shown.

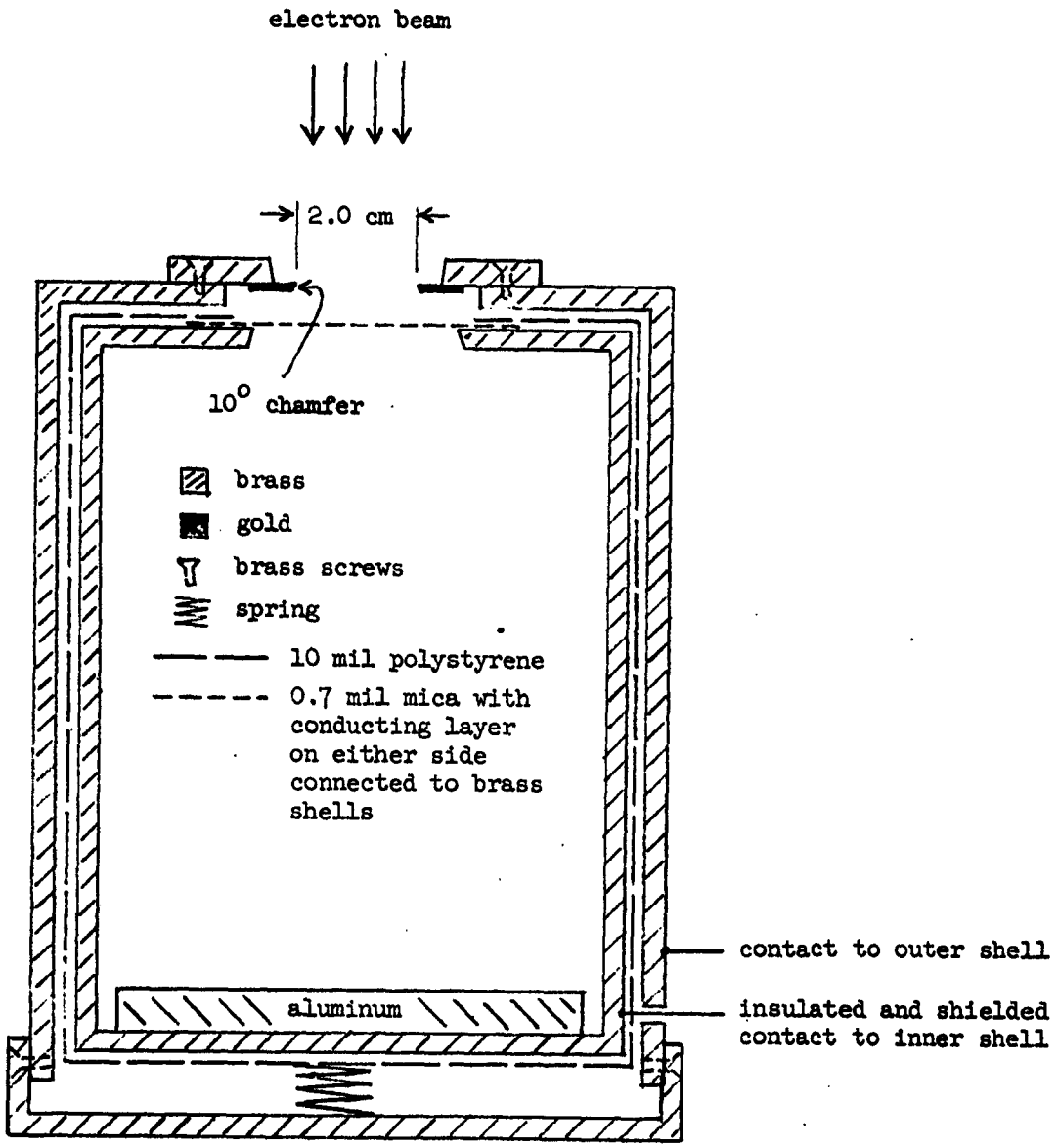

Figure 13. Cross Section of Faraday Cup to Full Scale. Gold collimating plate and mica window are replaceable. The structure has square symmetry.

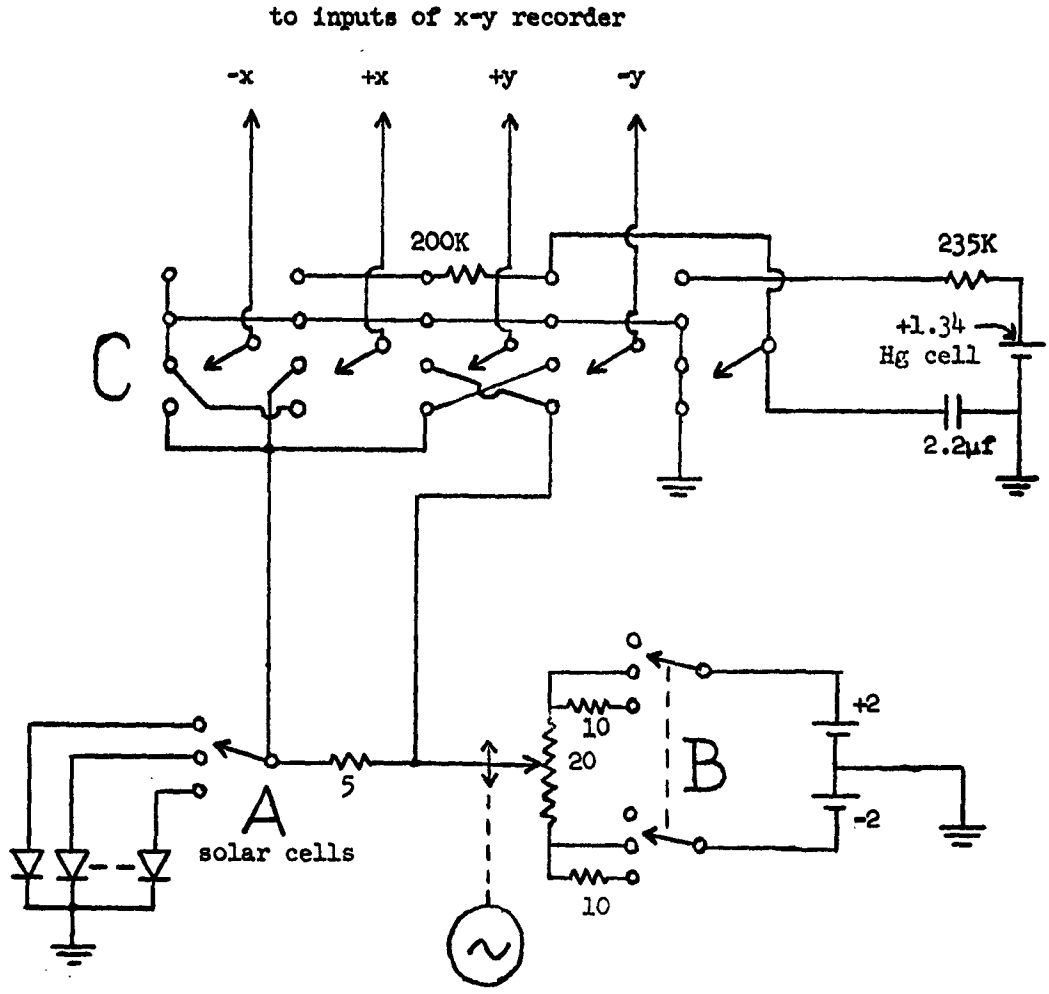

Figure 14. Circuitry Used to Measure I-V Characteristics. Switch A selects one solar cell. Switch B selects, from top down; power off, dark curve measurement, or power curve measurement. Switch C selects, from bottom up; measure p-type base cells, measure n-type base cells, calibrate zero position, and draw calibration line. Constant speed motor causes a full I-V curve to be drawn in six seconds. Resistance values are in ohms and voltages in volts.

DISTRIBUTION LIST

CYS	ACTIVITIES AT WPAFB
2	ASAPR (Library)
1	ASRPM
1	ASMPFS
1	ASRME-31 (Mrs. Tarrents)
5	ASRPP-20 (Mr. Wise)

OTHER DEPT OF DEFENSE ACTIVITIES

1	SSD (SSTRE, Maj Iller) AF Unit Post Office Los Angeles 45 Calif
15	DDC Arlington Hall Stn Arlington 12 Va
1	Dr. Fredrick Penzig, RRRS Office of Research Analyses OAR Holloman AFB, New Mexico
1	SSD (SSZAS, Maj G. Austin) AF Unit Post Office Los Angeles 45 Calif
1	Mr. George Hunrath SELRA/SL-PSP Energy Conversion Branch USAELRDL Ft Monmouth, New Jersey
1	Dr. E. L. Braneato Head Ins. Sect. Naval Research Laboratory Washington 25, D.C.
1	Mr. M. Cruseuße Naval Ordnance Test Station Code 3543 China Lake, California

Cys	
1	Mr. Milton Knight Bureau of Naval Weapons Code RAAE 5111 Department of the Navy Washington 25, D.C.

NASA

1	NASA Headquarters ATTN: Mr. Walter C. Scott 1512 H St NW Washington 25 D.C.
1	Mr. Atwood R. Heath Jr. NASA Langley Research Center Langley Field, Virginia
1	William R. Cherry Space Power Tech Branch NASA Goddard Space Center Greenbelt Maryland
1	NASA Manned Spacecraft Center SEDD (F. M. Plauche') Houston 1, Texas

NON GOVT INDIVIDUALS & ORGANIZATIONS

1	Aerospace Corporation ATTN: Library Technical Documents Gp P. O. Box 95085 Los Angeles 45, California
1	Jet Propulsion Laboratory California Institute of Technology ATTN: Arvin Smith 4800 Oak Grove Drive Pasadena, California
1	Robert Fischell Power Systems and AA Cont. JHU/Applied Physics Lab Silver Spring, Maryland
1	Radiation Effects Information Center Battelle Memorial Institute 505 King Avenue Columbus 1, Ohio

TECHNICAL DOCUMENT SUMMARY (TDS) CARD

The TDS card is the basic tool for indexing and retrieving technical information throughout Westinghouse. The 3 x 5 card cutouts provide for filing by numbers and subjects. Authors should prepare a TDS card for every significant technical report, memorandum and patent disclosure. Instructions "Keywording Westinghouse Reports" are available from Central Laboratories Administrative Services. Reports are distributed by the issuing department; for a copy use the pre-addressed request cutout card. Discard TDS cards not of interest. Issuing department assigns TDS numbers according to its system. For a retrieval system, new accession numbers and additional keywords may be necessary for which space is reserved on the back. A space for major subject heading (abbreviated "Class.") is included. It should indicate areas of interest such as bearings, transformer insulation, steam turbines.

TO Engineering Center
Radiation & Nucleonics Lab.

TDS- RR 63-927-534-R1

Send Copy of Document to:

Send TDS Card to:

TDS- 63-927-534-R1 Research Report

Class. Radiation Damage to Dendritic Solar Cells

WEBBED DENDRITIC SILICON SOLAR CELL RADIATION EFFECTS INVESTIGATION - QUARTERLY PROGRESS REPORT FOR THE PERIOD JANUARY 15 - APRIL 15, 1963*, K. S. Tarneja,[1] R. V. Babcock[2] R. D. Lamb,[1] p. 35.

Keywords - solar-cells, silicon, photovoltaic, dendrites, radiations, radioactive, semiconductors, diodes, energy, space, damage, junctions, depth, resistance.

This report discusses initial work toward maximizing the radiation resistance of silicon webbed dendritic solar cells. Design considerations, techniques for fabricating cells of 1 Ω cm resistivity, and steps preparatory to radiation damage study are presented. Efficiencies as high as 12.4% have been achieved on solar cells made from 1 Ω-cm n-type silicon webbed dendrites. (over)

TO Engineering Center
Radiation & Nucleonics Lab.

TDS- RR 63-927-534-R1

Send Copy of Document to:

Send TDS Card to:

TDS- 63-927-534-R1 Research Report

Class. Radiation Damage to Dendritic Solar Cells

WEBBED DENDRITIC SILICON SOLAR CELL RADIATION EFFECTS INVESTIGATION - QUARTERLY PROGRESS REPORT FOR THE PERIOD JANUARY 15 - APRIL 15, 1963*, K. S. Tarneja,[1] R. V. Babcock[2] R. D. Lamb,[1] p.35.

Keywords - solar-cells, silicon, photovoltaic, dendrites, radiations, radioactive, semiconductors, diodes, energy, space, damage, junctions, depth, resistance.

This report discusses initial work toward maximizing the radiation resistance of silicon webbed dendritic solar cells. Design considerations, techniques for fabricating cells of 1 Ω cm resistivity, and steps preparatory to radiation damage study are presented. Efficiencies as high as 12.4% have been achieved on solar cells made from 1 Ω-cm n-type silicon webbed dendrites. (over)

TO Engineering Center
Radiation & Nucleonics Lab.

TDS- RR 63-927-534-R1

Send Copy of Document to:

Send TDS Card to:

TDS- 63-927-534-R1 Research Report

Class. Radiation Damage to Dendritic Solar Cells

WEBBED DENDRITIC SILICON SOLAR CELL RADIATION EFFECTS INVESTIGATION - QUARTERLY PROGRESS REPORT FOR THE PERIOD JANUARY 15 - APRIL 15, 1963*, K. S. Tarneja,[1] R. V. Babcock[2] R. D. Lamb,[1] p. 35.

Keywords - solar-cells, silicon, photovoltaic, dendrites, radiations, radioactive, semiconductors, diodes, energy, space, damage, junctions, depth, resistance.

This report discusses initial work toward maximizing the radiation resistance of silicon webbed dendritic solar cells. Design considerations, techniques for fabricating cells of 1 Ω cm resistivity, and steps preparatory to radiation damage study are presented. Efficiencies as high as 12.4% have been achieved on solar cells made from 1 Ω-cm n-type silicon webbed dendrites. (over)

*The research and development reported in this report has been made possible through support and sponsorship extended by the Flight Accessories Laboratory of the Wright Patterson Air Force Base, Ohio, under contract number AF 33(657)-10527.

[1]Special Products Section, Youngwood, Pa.

[2]Research Laboratories

Do Not Type Abstract Below This Line

*The research and development reported in this report has been made possible through support and sponsorship extended by the Flight Accessories Laboratory of the Wright Patterson Air Force Base, Ohio, under contract number AF 33(657)-10527.

[1]Special Products Section, Youngwood, Pa.

[2]Research Laboratories

Do Not Type Abstract Below This Line

*The research and development reported in this report has been made possible through support and sponsorship extended by the Flight Accessories Laboratory of the Wright Patterson Air Force Base, Ohio, under contract number AF 33(657)-10527.

[1]Special Products Section, Youngwood, Pa.

[2]Research Laboratories

Do Not Type Abstract Below This Line